

# Heights of SuperDARN F region echoes estimated from the analysis of HF radio wave propagation

A. V. Koustov<sup>1</sup>, D. André<sup>1</sup>, E. Turunen<sup>2</sup>, T. Raito<sup>2</sup>, and S. E. Milan<sup>3</sup>

<sup>1</sup>Institute of Space and Atmospheric Studies, University of Saskatchewan, 116 Science Place, Saskatoon, S7N 5E2 Canada

<sup>2</sup>Sodankyla Geophysical Observatory, Sodankyla, Finland

<sup>3</sup>University of Leicester, Leicester, UK

Received: 5 May 2007 – Revised: 7 September 2007 – Accepted: 14 September 2007 – Published: 2 October 2007

**Abstract.** Tomographic estimates of the electron density altitudinal and latitudinal distribution within the Hankasalmi HF radar field of view are used to predict the expected heights of F region coherent echoes by ray tracing and finding ranges of radar wave orthogonality with the Earth magnetic field lines. The predicted ranges of echoes are compared with radar observations concurrent with the tomographic measurements. Only those events are considered for which the electron density distributions were smooth, the band of F region HF echoes existed at ranges 700–1500 km, and there was a reasonable match between the expected and measured slant ranges of echoes. For a data set comprising of 82 events, the typical height of echoes was found to be 275 km.

**Keywords.** Ionosphere (Auroral ionosphere; Ionospheric irregularities; Wave propagation)

## 1 Introduction

The SuperDARN HF radars (Greenwald et al., 1995) are widely used for monitoring plasma convection at high latitudes. SuperDARN-derived convection maps are convenient for placing other measurements into a global context (e.g. Kozlovsky et al., 2002; Bristow et al., 2003). Convection estimates in localized areas are also useful for understanding various high-latitude phenomena (e.g. Lyons et al., 2003; Oksavik et al., 2006).

To produce a global-scale map of plasma convection, the velocity of SuperDARN echoes, measured by individual radars at various ranges and for one scan, are combined into a common data set. Every such data set is then analyzed by fitting the measured velocities to a startup model of the expected convection pattern (Ruohoniemi and Baker, 1998).

*Correspondence to:* A. V. Koustov  
(sasha.koustov@usask.ca)

In the course of fitting, each velocity vector is assigned to a specific location by assuming that the received echoes are coming from the height of 300 km, for all echoes available. It has been general understanding that the assumptions of a fixed height for F region SuperDARN echoes and a specific choice of 300 km are both seldom correct, though the errors involved are typically not significant (Andre et al., 1997). The echo location estimates for artificially produced irregularities confirms this opinion, to some extent (Yeoman et al., 2001).

It is obvious that for accurate mapping of the echo location (convection vectors placement) in general case, information on the echo heights would be advantageous. Echo height estimates can be made from measurements of the elevation angle of echo arrival (e.g. Milan and Lester, 1999). Such estimates, however, are still prone to significant uncertainties because, for proper ray tracing at HF, at least two-dimensional (2-D) distribution of the electron density in the ionosphere needs to be specified for every radar beam position.

In this study an attempt is made to statistically estimate the expected heights of F region echoes by considering HF ray paths to the scattering area and by matching the predicted ranges of the echo detection to the observed ranges. For ray tracing, tomographic estimates of 2-D distribution of the electron density in the ionosphere are used.

## 2 SuperDARN echo height estimates from concurrent radar-tomography data

We first consider one specific event to describe how HF echo heights have been inferred from tomography and radar data.

### 2.1 Hankasalmi radar observations and events selection criteria

The SuperDARN radar antennas have a broad lobe in a vertical plane so that signals can be received in a range of

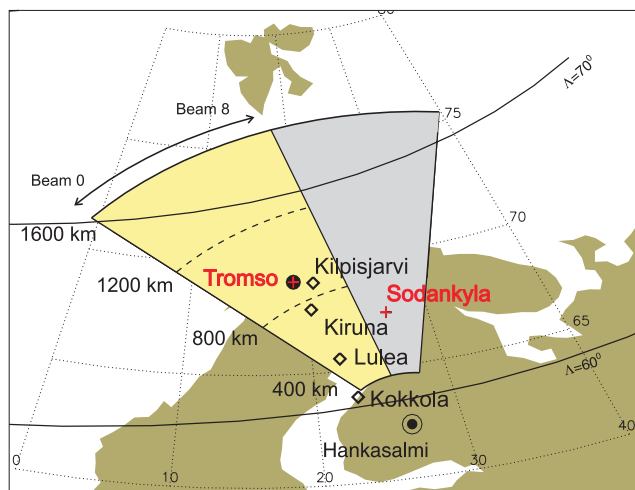


**Fig. 1.** Field of view of the Hankasalmi HF radar between 400 km and 1600 km and locations of the scintillation receivers (Kokkola, Lulea, Kiruna and Kilpisjarvi) used for tomography derivations of the electron density distribution in the ionosphere.

elevation angles, at least between  $\sim 5^\circ$  and  $\sim 50^\circ$  (e.g. Arnold et al., 2003). As transmitted radio waves propagate through the ionosphere, they refract and some of them can reach orthogonality to the magnetic field lines. Such waves have a chance to be backscattered if ionospheric irregularities of proper size exist at ranges of orthogonality. In this study we postulate that once a radar wave is within  $\pm 1^\circ$  of off-orthogonality with the Earth magnetic field line, the returned signal is detected. This postulate implies that the ionospheric irregularities exist at all F region heights and that the irregularities effectively backscatter the HF radio waves even though they are not exactly elongated with the magnetic field lines. We assume that the irregularities exist anywhere between 150 km and 500 km.

SuperDARN radars record information on the echo range, power, velocity and spectral width (Greenwald et al., 1995) obtained from the main antennae array. An additional (interferometer) array provides estimates of the elevation angle of echo arrival. In this study, we do not consider the widths and velocity of the echoes with the exception that both parameters are used to identify the ionospheric echoes.

In this study, we consider observations by the Hankasalmi HF radar over Northern Scandinavia. Figure 1 shows a part of this radar field-of-view (FoV) between ranges of 400 and 1600 km. In the standard mode of operation, the radar scans through 16 beam positions covering a segment-like area, as shown in Fig. 1. Echoes received in beams 0 to 8 and at ranges 400–1600 km (yellow segment) are considered. This is because the tomographic images of the 2-D electron density distribution in the ionosphere were only available for this part of the Hankasalmi radar FoV. To better explain this point, we show in Fig. 1 by diamonds the locations of

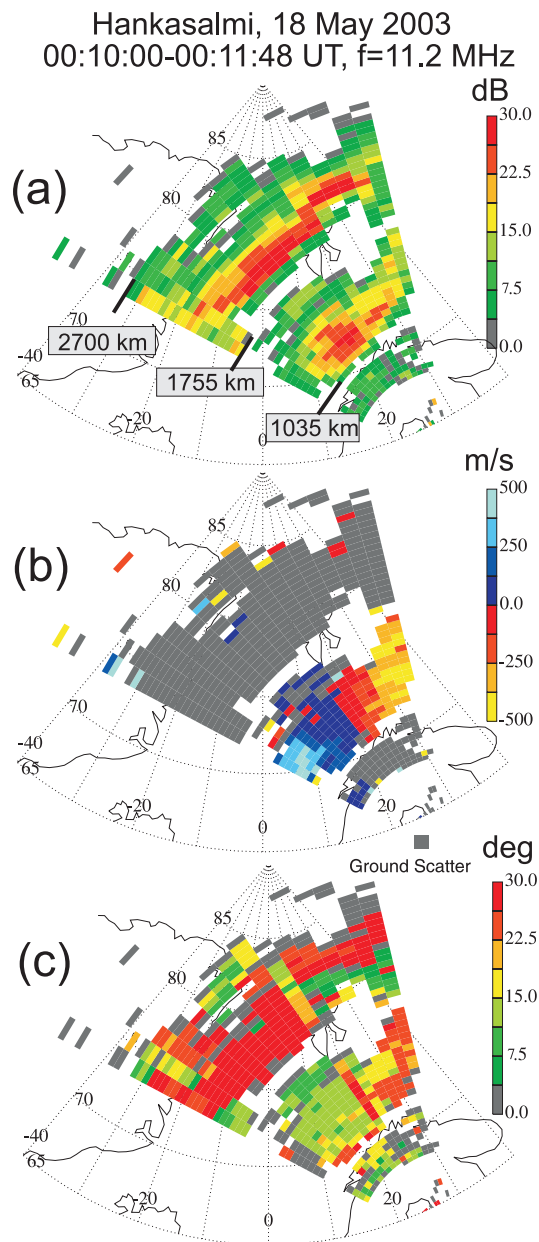


**Fig. 2.** Hankasalmi echo maps for (a) the power, (b) Doppler velocity and (c) elevation angles on 18 May 2003 between 00:10 and 00:12 UT. Frequency of operation was 11.18 MHz.

the scintillation receivers at Kokkola ( $63.83^\circ$  N,  $23.06^\circ$  E), Lulea ( $65.58^\circ$  N,  $22.17^\circ$  E), Kiruna ( $67.84^\circ$  N,  $20.41^\circ$  E) and Kilpisjarvi ( $69.02^\circ$  N,  $20.86^\circ$  E). One can see that the tomography coverage is available for beams 0–8 and for slant ranges from Hankasalmi between  $\sim 400$  km and  $\sim 900$  km. We add that the tomography measurements are actually available for broader area in terms of latitude because the satellites fly roughly along the magnetic meridian and at heights above 500 km so that useful signals for processing begin to be received at elevation angles well off the zenith of each

station allowing density estimates somewhat equatorward of Kokkola (up to 200 km) and poleward of Kilpisjärvi (up to ranges of  $\sim 1800$  km).

It is important to know that Hankasalmi echoes received at ranges of 400–900 km are quite often coming from the E region, sometimes from the F region and sometimes from both the E and F regions (Milan and Lester, 1999). At farther ranges of 900–1500 km, the echoes are usually coming from F region heights. All these types of echoes are expected to be received via the  $1/2$  hop propagation mode, i.e. direct radio wave propagation to the scattering area with appropriate amount of refraction. Separation of echo types for each scan is not a simple task; sometimes it can be done by looking at elevation angle information but for many events considered it was not straightforward. In this study, we considered only those events for which we were able to separate E and F region scatter confidently. To accomplish this, we first of all were seeking events at ranges  $>700$  km and we used all available information, such as spatial distribution echo parameters, elevation angles and distribution of the electron density.

Figure 2 gives an example of echoes received by the Hankasalmi radar on 18 May 2003 between 00:10 and 00:12 UT. Figure 2a shows that the echoes were received from three bands centered at about 800 km, 1300 km and 2200 km. The bands are well defined; the echo bands at far and close ranges are classified as ground scatter by the standard SuperDARN software, Fig. 2b. However, we believe that the short range echoes are actually the ionospheric scatter from the E/upper D regions. Similar observations and interpretation have been presented by Uspensky et al. (2001). Our judgment is also supported by the low values of the elevation angle presented in Fig. 2c. Echoes at the middle ranges are F region  $1/2$  hop scatter (these have slightly larger elevation angles than the short range echoes). The present study deals with this type of echo. It is interesting to note that elevation angles for these echoes are largest at the near edge of the echo band and smoothly decrease with range, Fig. 2c, as one would expect if the height of echo is the same at all ranges. Figure 2 also shows a band of ground scatter at the farthest ranges. These are beyond the ranges of interest in this study, but we would like to make a note that the elevation angles for some of them are low, in the range of  $10^\circ$ – $15^\circ$ , corresponding to the elevation angles of E and F region scatter. This fact indicates that these echoes are received by means of one full hop propagation mode via the F region. Some echoes, however, show elevation angles of the order of  $25^\circ$ . These are very likely obtained through the back (or side) lobe of the Hankasalmi antennae (Milan et al., 1997) though such a judgment is difficult to justify. We will show the ray tracing diagram for this event in Fig. 3 to confirm that reception of echoes at large elevation angles and from forward direction is unlikely.

The example of Fig. 2 gives a sense as to what kind of radar observations were selected for comparison with ray tracing. It was initial intent of this study to use only events with more or less clearly identifiable echo bands so that F

region backscatter at low and high ranges could be resolved confidently. It turned out that finding such events was not an easy task because concurrent data on the electron density distribution of reasonable quality were not so frequent.

## 2.2 Tomographical determination of the 2-D density profiles and event selection

The tomographic method of the 2-D electron density distribution determination in the ionosphere has been described by Kunitsyn and Tereshchenko (2003) in general and by Markkanen et al. (1995) and Nygren et al. (1997) with respect to the network of scintillation receivers considered in the present study. In short, a chain of several (four in our case) satellite receivers observed signals from Russian Low Earth Orbit satellites. Two signals transmitted coherently at frequencies 150 MHz and 400 MHz were received and their phase difference was used to calculate the ionospheric electron density by means of statistical inversion. A procedure was designed that fits the observed phase values to the startup model of the 2-D electron density distribution. Routine estimates were performed by applying two models of the electron density distribution, one was based on a Chapman layer with a peak height at 280 km and another one was based on the IRI model (Bilitza et al., 1997) density distribution over Kokkola shifted down by 50 km. In this study we adopted the IRI-based density distribution estimates; these often show reasonable agreement with concurrent measurements by independent instruments such the EISCAT radar (Nygren et al., 1996). For this choice of startup model, a boundary condition was that the electron density was zero at the ground level. The results of the regularization procedure were presented in terms of the electron density distribution in a vertical plane above the receiver chain. In an ideal case, the satellite would fly in a vertical plane along the chain. For most of passes considered in this study, however, the satellites were off this plane. In these cases, the obtained densities were a projection from regions outside the vertical plane. Because electron density measurements were not obtained exactly along the Hankasalmi meridian, a concern can be raised on the validity of the density distributions. We would like to mention that in this study we consider large-scale characteristics of echo regions and data in multiple radar beams so that the tomography uncertainties should not obscure the major features of the ionosphere that are important for HF signal.

A sequential search through 2 years of Hankasalmi radar and tomography data, 2003 and 2004, was performed to find appropriate events. It should be remembered that because only 4 receivers were available for the period under study, the electron density distributions were available for limited latitude over Northern Scandinavia and limited slant ranges of the Hankasalmi radar, see Fig. 1. In terms of the radar observations, slant ranges between 400 and 1600 km were covered completely by the tomography, and somewhat limited coverage was achieved for slant ranges of 1600–1800 km. We

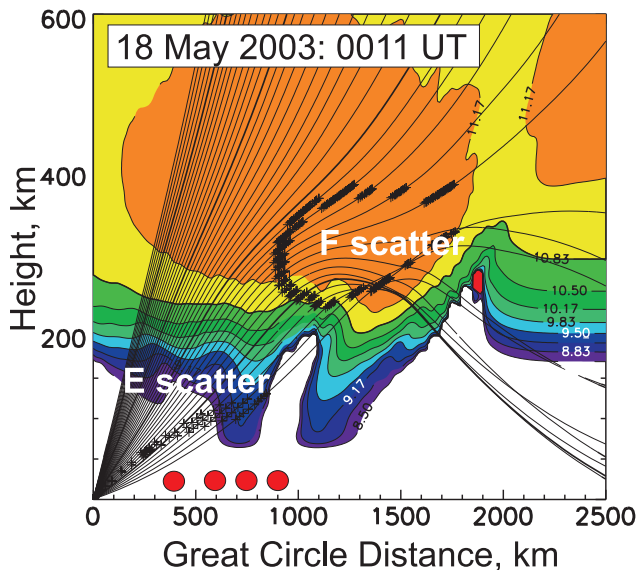


**Fig. 3.** Electron density distribution along the scintillation receivers meridian and the 2-D ray tracing for the Hankasalmi beam 5 and the event of 18 May 2003, 00:11 UT. Red disks indicate approximate locations of the scintillation receivers. The color coding for the density contours is as follows: blue – between  $3.16 \times 10^8 \text{ m}^{-3}$  and  $6.76 \times 10^9 \text{ m}^{-3}$ ; green – between  $6.76 \times 10^9 \text{ m}^{-3}$  and  $6.76 \times 10^{10} \text{ m}^{-3}$ ; yellow – between  $6.76 \times 10^{10} \text{ m}^{-3}$  and  $1.48 \times 10^{11} \text{ m}^{-3}$ ; brown – above  $1.48 \times 10^{11} \text{ m}^{-3}$ . Rays are shown in  $1^\circ$  step of elevation angle starting from  $5^\circ$ . The thicker traces correspond to elevation angles of  $10^\circ$ ,  $20^\circ$ ,  $30^\circ$  and  $40^\circ$ .

would like to warn the reader that even though the data above 1800 km will be shown, their relevance to the real situation is unknown and we will refrain from comments on radar wave trajectories at ranges  $> 1800$  km.

The search for potential events included several steps. First, general quick review of the tomography data on the Sodankyla Geophysical Observatory Web site (<http://www.sgo.fi>) was performed. Generally, quite a few potentially good events for every day were identified. We sought events with clear and smooth “walls” or boundaries in terms of latitude since, for such events, the correlation with HF echo occurrence was found to be more obvious. Events at short ranges  $\sim 500$ – $700$  km were generally not considered as it was difficult to distinguish E region and F region echo boundaries so that the backscatter height determination was not obvious (see description later). We also avoided observations for which the ionosphere consisted of several density blobs potentially leading to a complicated pattern of radar rays in the ionosphere and difficulty in assigning a typical height of an HF echo.

### 2.3 F region echo height determination

Once joint radar-tomography events were identified, estimates of the most likely height of F region echoes were performed. To accomplish this task, ray tracing for the Hankasalmi radar was performed by assuming 2-D electron density distribution (as given by the tomography) for the azimuth of  $15^\circ$  west of the geographic meridian which would correspond roughly to the Hankasalmi beam #6 location. The transmitted frequency in each event was taken into account.

For tracing of the rays we used a program that is based on the Cartesian form of the ray equations developed by Haselgrove (1963); the Runge-Kutta algorithm for solving the differential equations was taken from Press et al. (1986). The algorithm uses an adaptive stepsize to reduce the amount of calculations. The program takes into account the wave group delay.

The measured electron density was accepted as a two-dimensional table with values in height and distance from the radar. Interpolation to locations between the table values was done using two-dimensional spline interpolation (also taken from Press et al., 1986), because the tracing program needs both the electron density and its gradient to be without discontinuities. Finally, the IGRF magnetic field model was used for the aspect angle calculations.

Figure 3 illustrates the analysis. In this diagram, the background colored contours describe the electron density distribution in the ionosphere produced by particle precipitation (the events occurred in the dark ionosphere). Horizontally, the great circle distance is used. One can see a large-scale blob of enhanced density between the radar ranges of 200 km and 1800 km. The density inside this blob is above  $1.48 \times 10^{11} \text{ m}^{-3}$ ; the maximum values are of the order  $3.2 \times 10^{11} \text{ m}^{-3}$ . To check the reliability of the tomographic density estimates we considered the ionosonde data collected at Sodankyla (Hankasalmi ranges of  $\sim 650$  km). According to Sodankyla ionosonde, the  $f_oF_2$  frequency was 5.1 MHz (at the closest time) which corresponds to the density of  $3.2 \times 10^{11} \text{ m}^{-3}$ . Although this value coincides with the maximum electron density inferred from the tomographic measurements, we should mention that the density maximum according to tomography was achieved at ranges of  $\sim 1000$  km from Hankasalmi. At ranges of Sodankyla ionosonde location ( $\sim 650$  km), the density was somewhat smaller,  $2.5 \times 10^{11} \text{ m}^{-3}$ . We attribute this rather small difference to the longitudinal separation for the areas of the tomographic and ionosonde measurements and some errors in tomography analysis.

In Fig. 3, electron density decreases strongly toward lower heights so that at  $\sim 200$  km it is of the order of  $10^{10} \text{ m}^{-3}$ ; such densities do not affect the Hankasalmi radio wave paths significantly. Figure 3 also shows paths of various rays in the ionosphere taking off at elevation angles  $\varepsilon$  of  $5$ – $45^\circ$ . The traces for  $\varepsilon = 10^\circ$ ,  $20^\circ$ ,  $30^\circ$ , and  $40^\circ$  are shown by thicker line to facilitate the diagram overview. Each cross along a ray

trace indicates that part of the ray trajectory where the ray is within  $\pm 1^\circ$  of the off-orthogonality condition thus signifying a possibility of echo detection at this specific range. One can notice a cloud of crosses at ranges of 200–800 km and heights of 50–120 km and a horse-shoe like cloud of crosses at ranges 900–1800 km and heights of 230–350 km. These two clouds are the expected locations, in range and height, of E region echoes (between 90 and 120 km) and F region echoes.

Figure 3 shows that F region echoes can come from quite a range of heights and great circle distances. An important feature of the prediction is that echoes are expected at all ranges from 900 km up to 1800 km, in terms of the great circle distance. These numbers should be increased by 50–150 km, if the distances are counted in terms of the radar slant range. Actual radar data show that the echoes cover the band of 1035–1755 km, Fig. 2, for the scan under consideration. The range extension of the band is 720 km and the band's short range border is shifted poleward by  $\sim 85$  km from what is predicted. We attribute this shift to a slight error in tomographic electron density estimates and decide that only ranges from 950 to  $950+720=1670$  km have to be considered in model estimates of the scatter height. The predicted potential scatter from farther ranges of 1670 km (once again, used in Fig. 3 great circle ranges are shorter than slant ranges of echoes, see also later Fig. 4) is not counted as the observation does not show such echoes. Similar consideration and judgment were applied for each individual event; the differences between the model predictions and measurements at the shortest ranges of an echo band of up to 100 km were allowed. We admit that the procedure of echo ranges cutoff is somewhat subjective.

Figure 4 explains how the “typical” height was determined for each individual event. Here we show the slant ranges, the actual ranges along curved trajectories (Fig. 3 uses great circle distance which can be up to  $\sim 100$  km shorter) and the heights of expected orthogonal intersections according to ray tracing of Fig. 3. We also show by red circle every point which is within the band of possible slant ranges of echoes according to radar measurements. There are 183 such points. The median value for the height of all these points (horizontal line in Fig. 4) was considered to be the most likely height of F region echoes. For this specific event, this value turned out to be 297 km. We also computed the average height for crosses with red circles in Fig. 4; the average height was found to be 306 km. This is a very typical situation that the mean and median values do not differ much.

We should mention that the median value was counted for all crosses located between heights of  $h_{\min}=150$  km and  $h_{\max}=500$  km, the assumed height range of the irregularity layer. For the event under consideration, the orthogonality condition was met in rather limited band of heights. To characterize the height extent of echo region, we computed the difference between the lowest and highest points for each diagram; for the 18 May 2003 event, it was  $\sim 149$  km. We call this parameter the thickness of the backscatter layer.

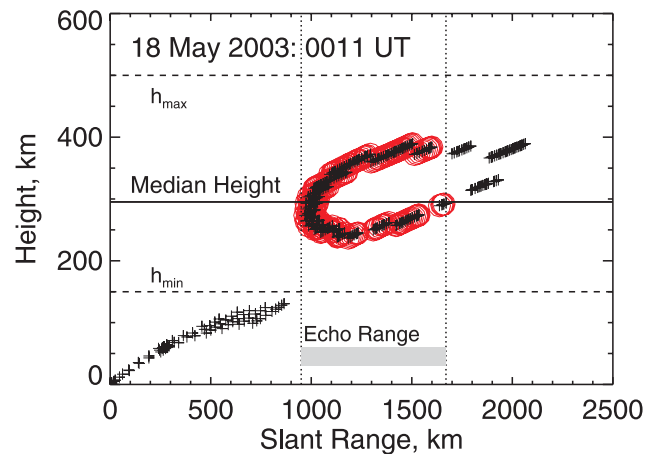


**Fig. 4.** Diagram illustrating the method of echo height estimation for the event of 18 May 2003, 00:11 UT.

One can also notice that, according to Figs. 3 and 4, at some ranges the echoes are expected to come from two ionospheric heights with significantly different elevation angles. This expected feature of HF echo detection was discussed by Andre et al. (1997) and earlier by Uspensky et al. (1994) with respect to the E region observations. We note that expected elevation angles for the top and bottom parts of the scattering layer are largest at shorter ranges and decrease with range, Fig. 3. The effect is more pronounced for the echoes coming from the bottom part of the scattering layer. Actual radar data of Fig. 2 do show the elevation angle decrease clearly, as mentioned earlier, but whether the scatter is coming from two heights is difficult to judge from the data available. The fact that the elevation angles fall very quickly with range in Fig. 2 gives a hint that perhaps the top part of the expected scattering layer is less effective. This implies that the height estimates presented below are perhaps the upper limit of possible heights.

## 2.4 Statistical results

A systematic search through joint radar-tomography data base allowed us to identify 82 events for which determination of the most likely F region echo height was possible. Figure 5 summarizes our findings for (a) the height and (b) the thickness of the backscatter layer. The distribution for the echo height in Fig. 5a has a bell-like shape, slightly skewed toward smaller heights. The distribution peaks at  $\sim 280$  km, and the average height is 275 km. In individual cases, the height can be below 200 km and above 350 km. Distribution for the backscatter thickness is more uniform; there is about equal possibility of thickness between 10 and 150 km with somewhat preferential values of 120–130 km.

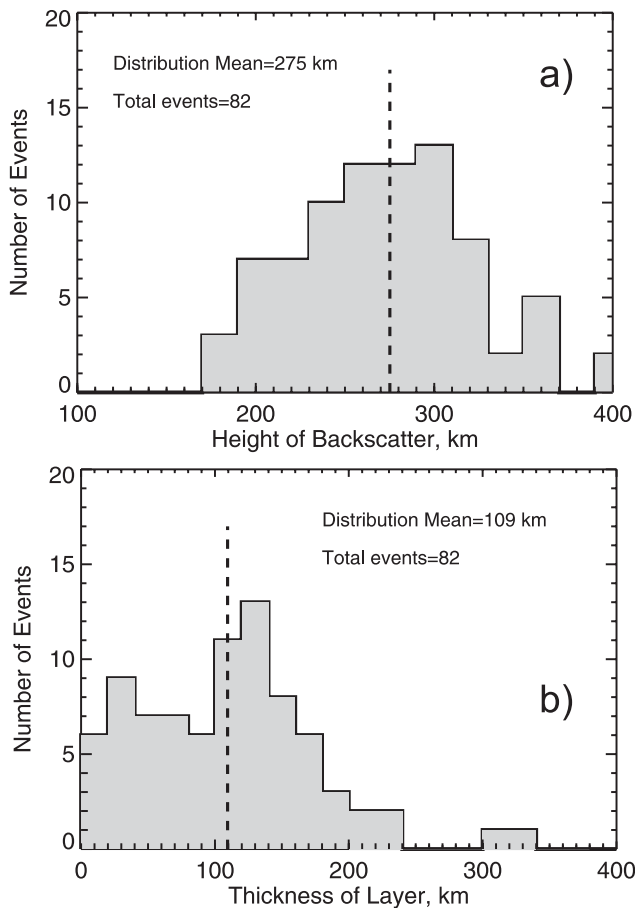


**Fig. 5.** Histogram distributions for (a) the heights of  $1/2$  hop propagation F-region echoes and (b) the altitudinal spread of expected echo heights (thickness of backscatter layer) for the entire data set of 82 events.

### 3 Discussion and summary

Measurements of the height of SuperDARN HF echoes is a challenging problem, and so far not much has been established. Previous ray tracings showed that HF radars are very sensitive to the electron density distribution in the ionosphere so that perpendicularity with the magnetic field lines can be achieved over a broad range of heights (Villain et al., 1984; Andre et al., 1997; Danskin, 2003). Villain et al. (1984) expected typical heights of more than 300 km while Danskin et al. (2002) and Danskin (2003) predicted rather low heights of <250 km. These previous studies suggest that the  $1/2$  hop F region scatter is typically coming from heights below the F region density peak. Milan and Lester (2001) presented estimates of the apparent F region echo heights using Hankasalmi interferometer data. Their Fig. 1 shows preferential heights of 220–230 km. The real heights in this experiment should be even smaller, implying fairly low F region echo heights. It is important to realize that these observations were performed, most likely, at short ranges as the experi-

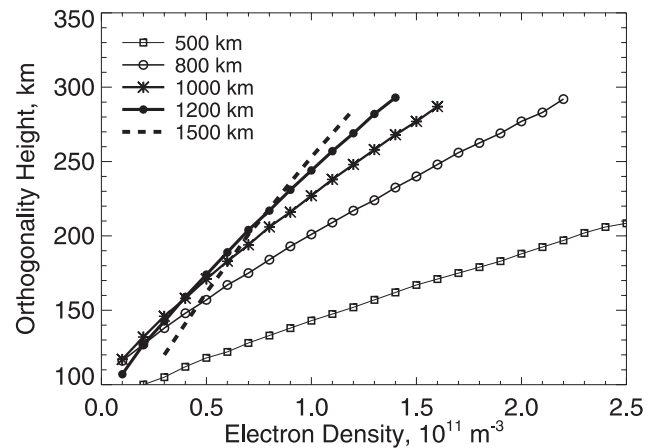


**Fig. 6.** Heights of the orthogonality condition (with refraction taken into account) for the Hankasalmi radar at ranges 500, 800, 1000, 1200 and 1500 km. A uniform electron density distribution, both horizontally and vertically, is assumed.

ment was run in the so called “myopic mode” with range bins of 15 km instead of standard 45-km bins. All the above predictions and measurements indicate great variability in the height of F region backscatter at HF; this is very likely because of the highly variable electron density distribution in the auroral zone (especially during frequent particle precipitation events) and also because the irregularities might exist in certain layers rather than throughout the entire F region.

Milan et al. (1999) established and later Danskin et al. (2002) confirmed that Hankasalmi  $1/2$  hop F region echoes near EISCAT (ranges  $\sim 900$  km) occur preferentially for the electron density of  $\sim 2 \times 10^{11} \text{ m}^{-3}$ . Simple ray tracing for vertically stratified (i.e. horizontally uniform) ionosphere for the Hankasalmi radar geometry shows that for such electron densities, the scatter should be coming from  $\sim 250$  km. To illustrate this point, we show in Fig. 6 the required densities at various heights so that the radar wave reaches orthogonality. Five ranges from Hankasalmi are considered. One can see, quite generally, that for electron densities below  $1.5 \times 10^{11} \text{ m}^{-3}$  the echoes are expected to come mostly from the heights <250 km over a broad band of ranges 800–1500 km, including the range of EISCAT location. These are exactly the ranges of echoes that we considered in this study. With the electron density increase, echoes can be detected at shorter ranges and at heights below 200 km. Our re-examination of the data used in Fig. 5 showed that indeed for all reported low-height events of <210 km, the minimum echo ranges were below 900 km. This result implies that if one selects only short range Hankasalmi events, the histogram of Fig. 5 would maximize at much lower heights. We also should mention that in a case of two-layer scattering, as in the example of Fig. 3, the upper layer might not always be effective, as discussed earlier, implying that the estimated typical heights can be smaller. In this study, the events were

**Table 1.** Expected median heights of Hankasalmi echoes for a number of electron density distributions that are modifications of the one shown in Fig. 3.

Density	Nominal	R+	R–	P+	P–	R+P+	R+P–	R–P+	R–P–
1.0Ne	297	292	299	323	300	322	304	323	292
0.7Ne	302	301	304	344	268	342	269	338	272
1.13Ne	328	246	265	324	308	333	195	336	311

selected randomly, and we think that Fig. 5 gives at least a good first estimate of what are the typical heights of the Hankasalmi F region echoes at ranges 700–1500 km. The inferred “typical height” of F region echoes of 275 km supports the choice of 300 km for the height of echoes adopted in the SuperDARN processing software, including the Map Potential technique of Ruohoniemi and Baker (1998).

The Hankasalmi  $1/2$ -hop F region echo heights estimates reported in this study depend strongly on the quality of the electron density distributions provided by the tomographic measurements. Unfortunately, reliability of the tomographic inversion technique that was employed in this study is not well established. Nygren et al. (1996) presented data validating the method for a subset of data, but reliability of density distributions for any time remains unclear. For one thing, the density distributions obtained by employing different startup density distributions with height are somewhat different in magnitude as one can witness by viewing data on the Sodankyla website. We hope that additional criterion for data selection allowed us to select periods with reasonable tomographic estimates; namely, we selected only those events for which the expected ranges of HF echoes were about the same as the ranges of observed echoes. To evaluate impact of uncertainty in the electron density distribution measurements on obtained results we performed a series of ray tracings with electron density distributions that were modifications of the one presented in Fig. 3. We used this profile but shifted it away (R+) or towards (R–) the radar location by 111 km (one degree of latitude) or shifted it up (P+) or down (P–) by 30 km. Combinations of the range and height shifts were also considered. We then repeated ray tracings by assuming that the densities are increased (decreased) by a factor of 1.3 (0.7). Results of this analysis for the median height are presented in Table 1.

First row in Table 1 shows that shifting of the density distribution of Fig. 3 in range (by  $\pm 111$  km) or height (by  $\pm 30$  km) does not give significant change in the echo median height. It is 5–20 km from the nominal height of 297 km. Similar conclusion can be made for the density distributions with the reduced magnitude, second row, except maximum difference from the nominal height can be as large as  $\sim 45$  km, both ways, positive and negative. For the case of increased densities (by 1.3 times, third row in Table 1), change in the expected echo height is more prominent, up to 100 km, with the strongest change occurring for the profile shifted

away (change is  $297-246=51$  km) and away and down simultaneously (change is  $297-195=102$  km). The performed estimates indicate that if the electron densities were somewhat larger than the ones used in this study, then the overall expected height of Hankasalmi echoes of 275 km would be somewhat smaller, perhaps by  $\sim 10-30$  km.

This paper considered echo heights only in terms of propagation conditions. Milan et al. (1998) showed that statistically, irrespective of propagation conditions, dayside HF echoes occur preferentially within the auroral oval (where electric fields and plasma density gradients are both enhanced) implying that irregularity production is very important factor for echo detection. We considered only those events for which echoes were seen, and we were sure that irregularities did exist in the ionosphere. Less certain was the assumption that decameter irregularities existed at all F region heights where orthogonality condition was met. If this was not the case, our estimates of typical height might be erroneous. Unfortunately, not much is known in terms of the irregularity production heights. If one assumes that the gradient-drift instability (e.g. Tsunoda, 1988) is the main source of decameter F region irregularities, then one may expect irregularity production at just about any height as the instability conditions do not change much with the height. Basically, having enhanced electric field and steep enough electron density gradient are enough to set the instability going. Certainly, the key question is whether gradients are present at all heights and at any instant of time. In addition, the role of the other factors, such as presence of highly conducting E region, need to be evaluated. Joint radar-tomographic observations complemented with scintillation detection of F region irregularities could be useful for future studies.

Results of this study can be summarized as follows.

1. Ray tracing analysis based on tomographic estimates of the 2-D electron density distribution within the field of view of the Hankasalmi HF radar showed that the most likely height of the F region echoes received through  $1/2$  hop propagation mode at ranges 700–1500 km is  $\sim 275$  km. The typical thickness of the backscatter layer, inferred from the analysis of propagation conditions only, is of the order of 100 km.
2. In individual events, echo heights of more than 350 km and less than 200 km are possible.

- Cases of Hankasalmi radar F region echo detection at very short ranges of <700 km when the echoes are very likely to be a mixture of scatter from the bottom-side F region and the electrojet E region were not considered and require further investigation.

*Acknowledgements.* We thank the U of Leicester radar group (M. Lester, PI) that continuously operated the Hankasalmi HF radar and provided data used in this study. Help of L. V. Benkevitch in data processing is appreciated. This work has been supported by NSERC (Canada) grant to A. V. Koustov.

Topical Editor M. Pinnock thanks M. Uspensky and P. L. Dyson for their help in evaluating this paper.

## References

- Andre, R., Hanuise, C., Villain, J.-P., and Cerisier, J.-C.: HF radars: Multifrequency study of refraction effects and localization of scattering, *Radio Sci.*, 32, 153–168, 1997.
- Arnold, N. F., Cook, P. A., Robinson, T. R., Lester, M., Chapman, P. J., and Mitchell, N.: Comparison of D-region Doppler drift winds measured by the SuperDARN Finland HF radar over an annual cycle using the Kiruna VHF meteor radar, *Ann. Geophys.*, 21, 2073–2082, 2003, <http://www.ann-geophys.net/21/2073/2003/>.
- Bilitza, D.: International Reference Ionosphere: Status 1995/96, *Adv. Space Res.*, 20(9), 1751–1754, 1997.
- Bristow, W. A., Sofko, G. J., Stenbaek-Nielsen, H. C., Wei, S., Lummerzheim, D., and Otto, A.: Detailed analysis of sub-storm observations using SuperDARN, UVI, ground-based magnetometers, and all-sky imagers, *J. Geophys. Res.*, 108(A3), 1124, doi:10.1029/2002JA009242, 2003
- Danskin, D. W., Koustov, A. V., Ogawa, T., Nishitani, N., Nozawa, S., Milan, S. E., Lester, M., and André, D.: On the factors controlling occurrence of F-region coherent echoes, *Ann. Geophys.*, 20, 1385–1397, 2002, <http://www.ann-geophys.net/20/1385/2002/>.
- Danskin, D. W.: HF auroral backscatter from the E and F regions, PhD thesis, U of Saskatchewan, Saskatoon, SK, Canada, 2003.
- Greenwald, R. A., Baker, K. B., Dudeney, J. R., Pinnock, M., Jones, T. B., Thomas, E. C., Villain, J.-P., Cerisier, J.-C., Senior, C., Hanuise, C., Hunsucker, R. D., Sofko, G., Koehler, J., Nielsen, E., Pellinen, R., Walker, A. D. M., Sato, N., and Yamagishi, H.: DARN/SuperDARN: A global view of the dynamics of high-latitude convection, *Space Sci. Rev.*, 71, 763–796, 1995.
- Haselgrove, J.: The Hamiltonian ray path equations, *J. Atmos. Terr. Phys.*, 25, 397–399, 1963.
- Kozlovsky, A., Koustov, A., Lyatsky, W., Kangas, J., Parks, G., and Chua, D.: Ionospheric convection in the postnoon auroral oval: Super Dual Auroral Radar Network (SuperDARN) and Polar ultraviolet imager (UVI) observations, *J. Geophys. Res.*, 107(12), 1433, doi:10.1029/2002JA009261, 2002.
- Kunitsyn, V. E. and Tereshchenko, E. D.: Ionospheric tomography, Springer-Verlag, Berlin, 2003.
- Lyons, L. R., Liu, S., Ruohoniemi, J. M., Solov'yev, S. I., and Samson, J. C.: Observations of dayside convection reduction leading to substorm onset, *J. Geophys. Res.*, 108(3), 1119, doi:10.1029/2002JA009670, 2003.
- Markkannen, M., Lehtinen, M., Nygren, T., Pirttila, J., Henelius, P., Vilenius, E., Tereshchenko, E. D., and Khudukon, B. Z.: Bayesian approach to satellite radiotomography with applications in the Scandinavian sector, *Ann. Geophys.*, 13, 1277–1287, 1997, <http://www.ann-geophys.net/13/1277/1997/>.
- Milan, S. E., Jones, T. B., Robinson, T. R., Thomas, E. C., and Yeoman, T. K.: Interferometric evidence for the observation of ground backscatter originating behind the CUTLASS coherent HF radars, *Ann. Geophys.*, 15, 29–39, 1997, <http://www.ann-geophys.net/15/29/1997/>.
- Milan, S. E., T. K. Yeoman, T. K., and Lester, M.: The dayside auroral zone as a hard target for coherent HF radars, *Geophys. Res. Lett.*, 25, 3717–3720, 1998.
- Milan, S. E., Davies, J. A., and Lester, M.: Coherent HF radar backscatter characteristics associated with auroral forms identified by incoherent radar techniques: A comparison of CUTLASS and EISCAT observations, *J. Geophys. Res.*, 104, 22 591–22 604, 1999.
- Milan, S. E. and Lester, M.: A classification of spectral populations observed in HF radar backscatter from the E region auroral electrojets, *Ann. Geophys.*, 19, 189–204, 2001, <http://www.ann-geophys.net/19/189/2001/>.
- Nygren, T., Markkannen, M., Lehtinen, M., Tereshchenko, E. D., Khudukon, B. Z., Evstafiev, O. V., and Pollari, P.: Comparison of F-region electron density observations by satellite radio tomography and incoherent scatter methods, *Ann. Geophys.*, 14, 1422–1428, 1996, <http://www.ann-geophys.net/14/1422/1996/>.
- Nygren, T., Markkannen, M., Lehtinen, M., Tereshchenko, E. D., and Khudukon, B. Z.: Stochastic inversion in ionospheric radiotomography, *Radio Sci.*, 32, 2359–2372, 1997.
- Oksavik, K., Ruohoniemi, J. M., Greenwald, R. A., Baker, J. B. H., Moen, J., Carlson, H. C., Yeoman, T. K., and Lester, M.: Observations of isolated polar cap patches by the European Incoherent Scatter (EISCAT) Svalbard and Super Dual Auroral Radar Network (SuperDARN) Finland radars, *J. Geophys. Res.*, 111, A05310, doi:10.1029/2005JA011400, 2006.
- Press, W., Flannery, B., Teukolsky, S., and Vetterling, W.: Numerical recipes, the art of scientific computing, Cambridge University Press, 1986.
- Ruohoniemi, J. M. and Baker, K. B.: Large-scale imaging of high-latitude convection with Super Dual Auroral Radar Network HF radar observations, *J. Geophys. Res.*, 103, 20 797–20 811, 1998.
- Tsunoda, R. T.: High latitude irregularities: A review and synthesis, *Rev. Geophys.*, 26, 719–760, 1988.
- Uspensky, M., Eglitis, P., Opgenoorth, H., Starkov, G., Pulkkinen, T. and Pellinen, R.: On auroral dynamics observed by HF radar: 1. Equatorward edge of the afternoon-evening diffuse luminosity belt, *Ann. Geophys.*, 18, 1560–1575, 2001, <http://www.ann-geophys.net/18/1560/2001/>.
- Uspensky, M. V., Koustov, A. V., Sofko, G. J., Koehler, J. A., Villain, J.-P., Hanuise, C., Ruohoniemi, J. M., and Williams, P. J. S.: Ionospheric refraction effects in slant range profiles of auroral HF coherent echoes, *Radio Sci.*, 29, 503–517, 1994.
- Villain, J. P., Greenwald, R. A., and Vickery, J. F.: HF ray tracing at high-latitudes using measured meridional electron density distributions, *Radio Sci.*, 19, 359–374, 1984.
- Yeoman, T. K., Wright, D. M., Stocker, A. J., and Jones, T. B.: An evaluation of range accuracy in the SuperDARN over-the-horizon HF radar systems, *Radio Sci.*, 36, 801–813, 2001.